

# Fourier transform-based $k \cdot p$ method of semiconductor superlattice electronic structure

T. Mei<sup>a)</sup>

School of Electrical and Electronic Engineering, Nanyang Technological University, Singapore 639798

(Received 2 February 2007; accepted 17 July 2007; published online 13 September 2007)

With the periodic spatial domain Hamiltonian being expressed as a Fourier series, a simple and neat Hamiltonian in a Fourier domain is formulated. The Fourier transform-based  $k \cdot p$  approach is developed to calculate electronic structures of semiconductor heterostructures. Calculation of electronic structures is investigated with several quantum well examples and comparison is made between this approach and the finite difference approach. The formulation of the Fourier domain Hamiltonian for quantum dots is presented as well. © 2007 American Institute of Physics.  
[DOI: 10.1063/1.2776158]

## I. INTRODUCTION

In the effective mass approximation (EMA),<sup>1</sup> electron and hole energy states in a bulk crystal are determined by solving an eigenproblem using a bulk Hamiltonian  $\mathbf{H}$ .<sup>2</sup> A superlattice may have abrupt interfaces, or graded composition modulation without sharp interfaces. In the former case, the eigenfunctions are found by matching wave functions in each of the constituent materials at the superlattice interfaces.<sup>3</sup> In the latter, electronic states have to be calculated via numerical approaches since the explicit Hamiltonian  $\mathbf{H}(\mathbf{r})$  is spatially varying. Numerical methods such as the finite difference method (FDM)<sup>4-6</sup> and the finite element method (FEM)<sup>7</sup> have been developed for electronic structure calculation of superlattices. These numeric methods may also work for the superlattices with abrupt interfaces, whereas with<sup>4</sup> or without<sup>6</sup> specific consideration of the interface matching condition, no significant difference in results has ever been reported.

In a periodic superlattice, the envelope function can be approximated by a Fourier series. However, a similar treatment is applicable to the spatially varying Hamiltonian  $\mathbf{H}(\mathbf{r})$  as well. The Hamiltonian in a Fourier domain for the eigenproblem can be formulated in a simple and neat form using the Fourier series of the spatial domain Hamiltonian. For arbitrary periodic structures, Fourier series expansion is implemented numerically by fast Fourier transform (FFT). Therefore, no cumbersome calculation on integral or differential is involved. Since the eigenfunction and its derivative possess a continuity property natively, it is manifest that this method is applicable to the superlattices with abrupt interfaces. In this article, we present the multiband  $k \cdot p$  Fourier transform method (FTM). The formulas of the FTM are derived and the solutions in several examples are given for illustration. Comparison is made between the FTM and FDM as well. Finally, the formulation is further extended to the case of quantum dot (QD) superlattices. To achieve high accuracy, the FDM results in a very large Hamiltonian matrix, which is challenging to solve practically. For three-

dimensional heterostructures, complicated formulations in both the FDM and FEM make programming tasks challenging. In contrast, it is seen that the FTM is advantageous to overcome issues in these aspects.

## II. FORMULATION FOR QW SUPERLATTICE

For the electron wave function written as

$$\psi(\mathbf{r}) = \sum_v^V F_v(\mathbf{r})u_{0v}(\mathbf{r}), \quad (1)$$

where  $u_{0v}$  is the Bloch basis with lattice periodicity,  $V$  is the number of bands involved in the model, and  $F_v(\mathbf{r})$  is the envelope function, it has been shown<sup>8</sup> in EMA that the envelope function equation for heterostructures can be obtained from position-dependent bulk Hamiltonians  $\mathbf{H}(\mathbf{r};\mathbf{k})$  with several operations, such as replacing  $k_z$ -related terms into differential operators,

$$\mathbf{H}(\mathbf{r};\mathbf{k}_{\parallel},\hat{k}_z)\mathbf{F}(\mathbf{r}) = E\mathbf{F}(\mathbf{r}). \quad (2)$$

If the envelope function is expanded in plane waves, the eigenproblem can be solved in the form of integral-differential equations by utilizing the orthogonality of plane waves, which is to be discussed below.

For a quantum well (QW) superlattice, the envelope function is expanded in plane waves in  $z$ ,

$$\mathbf{F}(\mathbf{r}) = e^{ik_x x + ik_y y} (1/\sqrt{L}) e^{ik_z z} \sum_n \mathbf{c}_n e^{in\kappa z}, \quad (3)$$

where  $L$  is the period,  $\mathbf{c}_n = [c_1 c_2 \cdots c_8]_n^T$ ,  $\kappa = 2\pi/L$ , and  $-\kappa < k_z \leq \kappa$ . Only wave-vectors in the first Brillouin zone need be included in the expansion for uniqueness.<sup>9</sup> If there are  $N$  superlattice periods, the Born-Von Karman cyclic boundary conditions give

$$k_z = \frac{2\pi j}{NL}, \quad 0 \leq j < N.$$

The plane waves keep their forms of complex exponential functions after operation by the operators contained in the Hamiltonian, whereas complex exponential functions possess orthogonality. Therefore, potentially the computation

<sup>a)</sup>FAX: +65-67920415; electronic mail: etmei@ntu.edu.sg

will be simplified if the  $z$ -dependent Hamiltonian matrix is expanded in Fourier series as well,

$$\begin{aligned} \mathbf{H} &= \mathbf{H}^{(2)}(z)\hat{k}_z^2 + \mathbf{H}^{(1)}(z)\hat{k}_z + \mathbf{H}^{(0)}(z) \\ &= \left[ \sum_q \mathbf{H}^{(2)}(q)e^{iq\kappa z} \right] \hat{k}_z^2 + \left[ \sum_q \mathbf{H}^{(1)}(q)e^{iq\kappa z} \right] \hat{k}_z + \sum_q \mathbf{H}^{(0)} \\ &\quad \times (q)e^{iq\kappa z}. \end{aligned} \quad (4)$$

Denoting  $\langle f_2 | f_1 \rangle = (1/L) \int_L f_2^* f_1 dz$ , it can be derived from Eq. (2) that

$$\begin{aligned} &\left\langle e^{i(k_z+m\kappa)z} \left| \sum_{v=1}^V \sum_n \sum_q c_{vn} (H_{uv}^{(2)}(q)e^{iq\kappa z} \hat{k}_z^2 \right. \right. \\ &\quad \left. \left. + H_{uv}^{(1)}(q)e^{iq\kappa z} \hat{k}_z + H_{uv}^{(0)}(q)e^{iq\kappa z} \right) e^{i(k_z+n\kappa)z} \right\rangle \\ &= \langle e^{i(k_z+m\kappa)z} | E \sum_n \sum_{v=1}^V [c_{vn} e^{i(k_z+n\kappa)z}] \rangle, \end{aligned} \quad (5)$$

$$\begin{aligned} &\sum_{v=1}^V \sum_n c_{vn} \left\{ \sum_q \left[ \langle e^{i(k_z+m\kappa)z} | H_{uv}^{(2)}(q)e^{iq\kappa z} \hat{k}_z^2 | e^{i(k_z+n\kappa)z} \rangle \right. \right. \\ &\quad \left. \left. + \langle e^{i(k_z+m\kappa)z} | H_{uv}^{(1)}(q)e^{iq\kappa z} \hat{k}_z | e^{i(k_z+n\kappa)z} \rangle \right. \right. \\ &\quad \left. \left. + \langle e^{i(k_z+m\kappa)z} | H_{uv}^{(0)}(q)e^{iq\kappa z} | e^{i(k_z+n\kappa)z} \rangle \right] \right\} \\ &= E \sum_{v=1}^V \sum_n c_{vn}, \end{aligned} \quad (6)$$

where  $u=1,2,\dots,V$ . We adopted an eight-band  $k \cdot p$  Hamiltonian<sup>11</sup> in this work. With the Hermitian operation,  $Q\hat{k}_i f \rightarrow [Q\hat{k}_i f + \hat{k}_i(Qf)]/2$  and  $Q\hat{k}_i \hat{k}_j f \rightarrow \hat{k}_i(Q\hat{k}_j f) + \hat{k}_j(Q\hat{k}_i f)/2$  where  $\hat{k}_i \rightarrow -i\partial_i$  and  $\hat{k}_j \rightarrow -i\partial_j$ ,<sup>10</sup> we have

$$\sum_q \langle e^{i(k_z+m\kappa)z} | H_{uv}^{(0)}(q)e^{iq\kappa z} | e^{i(k_z+n\kappa)z} \rangle = H_{uv}^{(0)}(q = m - n), \quad (7)$$

$$\begin{aligned} &\sum_q \langle e^{i(k_z+m\kappa)z} | H_{uv}^{(1)}(q)e^{iq\kappa z} \hat{k}_z | e^{i(k_z+n\kappa)z} \rangle \\ &= \left( \frac{\kappa m + \kappa n}{2} + k_z \right) H_{uv}^{(1)}(q = m - n), \end{aligned} \quad (8)$$

$$\begin{aligned} &\sum_q \langle e^{i(k_z+m\kappa)z} | H_{uv}^{(2)}(q)e^{iq\kappa z} \hat{k}_z^2 | e^{i(k_z+n\kappa)z} \rangle \\ &= (\kappa m + k_z)(\kappa n + k_z) H_{uv}^{(2)}(q = m - n). \end{aligned} \quad (9)$$

Therefore, the equation for the eigenproblem can be written as

$$[M_{st}][c_t] = E[c_t], \quad (10)$$

where the matrix elements of Fourier domain Hamiltonian  $\mathbf{M}$  have the following expression:

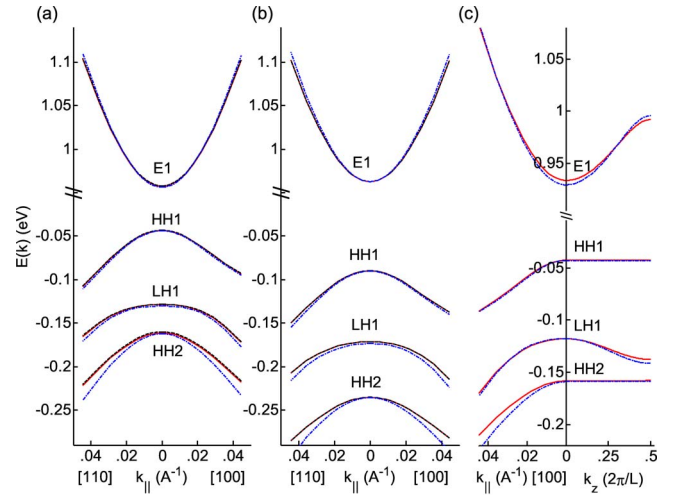


FIG. 1. (Color online) Bands of (a) AQW and (b) IQW in  $k$  space along [100] and [110] calculated using the FTM (—), FDM (---), and FTM with the approximation Eq. (12) (— · —) and bands of (c) SSL in  $k$  space along [100] and  $k_z$  calculated using the FTM with (— · —) and without (—) the approximation Eq. (12).

$$\begin{aligned} M_{st} &= (\kappa m + k_z)(\kappa n + k_z) H_{uv}^{(2)}(q) + \left( \frac{\kappa m + \kappa n}{2} + k_z \right) \\ &\quad \times H_{uv}^{(1)}(q) + H_{uv}^{(0)}(q), \quad q = m - n. \end{aligned} \quad (11)$$

The dimension of the Fourier domain Hamiltonian  $\mathbf{M}$  is determined by the number of the Fourier frequencies of  $\mathbf{H}$ . An arbitrary heterostructure may result in an infinite dimension of  $\mathbf{M}$ , but practically, for a periodic structure, the Fourier spectrum has negligible magnitudes at high frequencies and thus can be truncated. If the terms up to  $N$ th order in the Fourier series are retained for the wave function, i.e.,  $n, m = -N, \dots, 0, \dots, N$ , the Fourier series terms of  $\mathbf{H}$  will be reserved up to  $2N$ th order, i.e.,  $q = m - n = -2N, \dots, 0, \dots, 2N$ . Therefore, the dimension of  $\mathbf{M}$  is determined by the truncation frequency  $N$ , i.e.,  $V(2N+1) \times V(2N+1)$ . The subscripts for Eq. (11) can be schemed as  $s = u + V(m+N)$  and  $t = v + V(n+N)$ .

### III. ELECTRONIC STRUCTURE CALCULATION

To illustrate the FTM calculation, three structures are employed: a 35 Å  $\text{In}_{0.53}\text{Ga}_{0.47}\text{As}/300$  Å InP abrupt QW (denoted as AQW), a 35 Å  $\text{In}_{0.53}\text{Ga}_{0.47}\text{As}/300$  Å InP QW being intermixed with 5 Å diffusion length on both sublattices (denoted as IQW), and a short-period superlattice 35 Å  $\text{In}_{0.53}\text{Ga}_{0.47}\text{As}/40$  Å InP (denoted as SSL). The results obtained by the FTM are shown in Fig. 1 and the FDM results are presented as references in Figs. 1(a) and 1(b) as well. The calculation adopts the band parameters from Table I in Ref. 12. The QW structures are sliced with 512 mesh points for both FTM and FDM calculations. In the FTM calculation, a FFT is done with the mesh and the truncation frequency is  $N=20$  for forming the Fourier domain Hamiltonian. It is seen that the calculation results using these two methods agree with each other nicely.

In the FDM calculation, we did not have specific consideration of the interface matching condition for the reason stated as above. The FDM can incorporate the interface

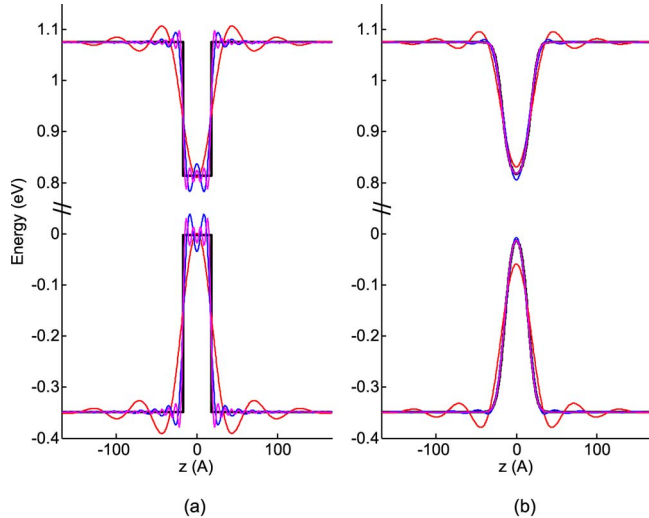


FIG. 2. (Color online) Spatial energy band edge profiles of (a) AQW and approximations in the Fourier series truncated to the 6th, 20th, and 40th orders and (b) IQW and approximations in the Fourier series truncated to the 6th, 10th, and 20th orders.

matching condition only for heterostructures with abrupt interfaces, e.g., AQW, but not for heterostructures with graded composition, e.g., IQW. For the circumstance of FTM, the interface matching condition cannot be intentionally incorporated because abrupt interfaces no longer exist in Fourier series approximation as shown in Fig. 2.

In some works, e.g., Ref. 13, the eigenvalue equation only adopts the bulk Hamiltonian of the QW layer's constitutional material and treats band offsets with a perturbation term in a form like

$$\mathbf{H}(z) = \mathbf{H}(0) + U(z), \quad (12)$$

where  $U(z)$  is diagonal in the basis and describes only the valence and conduction band offsets. The influence of such an approximation to accuracy can be evaluated in FTM calculation. The  $E-k$  plots in Fig. 1 show that the deviation due to this approximation goes large for large  $k_{\parallel}$ . A basic understanding is that such an approximation neglects the spatial variation of the band parameters, i.e.,  $\gamma_1$ ,  $\gamma_2$ ,  $\gamma_3$ ,  $E_p$ , and  $\Delta$ , and brings an appreciable error when band mixing goes large, i.e., large  $k$ . However, for a short-period superlattice, since the envelope function is not small over the barrier region, neglecting the spatial variation of band parameters will bring an appreciable deviation even at  $k=0$ . The  $E-k$  plot of SSL in Fig. 1(c) shows  $\sim 4$  meV deviation in  $E_1$  at  $k=0$ .

Under EMA, the FTM is derived without extra approximations or assumptions. However, for numerical calculation, a structure has to be meshed for performing a FFT if analytical expressions of the Fourier series are neither available nor adopted. Furthermore, the Fourier series need be truncated to make finite the Fourier domain Hamiltonian  $\mathbf{M}$ . Both meshing and truncation are factors causing numerical errors. Unlike the FDM, increasing mesh density does not cause a significant rise of the computing volume in the FTM, owing to the specific feature of the FFT algorithm. In comparison to the discretization-caused numerical error, which can be easily reduced, it takes more cost to reduce the truncation-caused numerical error. In Fig. 2, we can see that the trun-

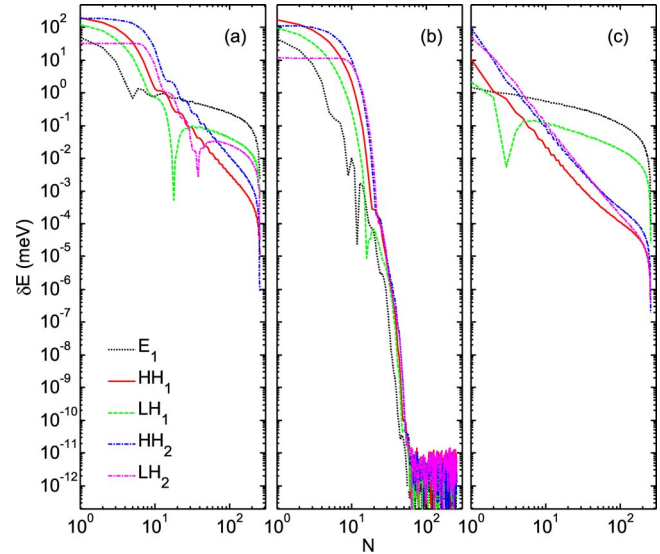


FIG. 3. (Color online) Truncation-caused numerical errors of the eigensolutions ( $k_{\parallel}=0$ ) versus the truncation frequency  $N$  for (a) AQW, (b) IQW, and (c) SSL.

ated Fourier series deviates from the original band edge profile, and the influences are different between heterostructures with abrupt interfaces and those with graded compositions. As shown in Fig. 3, to reach an accuracy of  $\sim 1$  meV, the truncation frequency  $N$  should be no less than 20, 14, and 5 for AQW, IQW, and SSL, respectively. The reason why the greatest  $N$  is needed for AQW but the smallest  $N$  for SSL to reach the same accuracy can be explained using the Fourier spectra shown in Fig. 4. AQW has a widespread spectrum compared to the others, whereas the spectrum of SSL has very large magnitudes only at the first several frequencies. The spectrum of IQW has the narrowest span, and thus the best accuracy can be achieved when  $N$  further increases, as seen in Fig. 3(b). A 512-point mesh is used to perform a FFT for the plots in Fig. 3.

Discretization-caused numerical error is investigated in

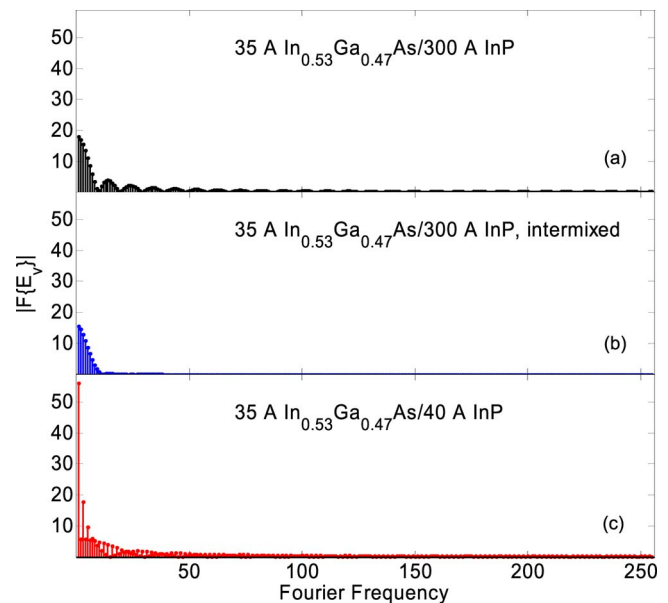


FIG. 4. (Color online) Fourier spectra for (a) AQW, (b) IQW, and (c) SSL.

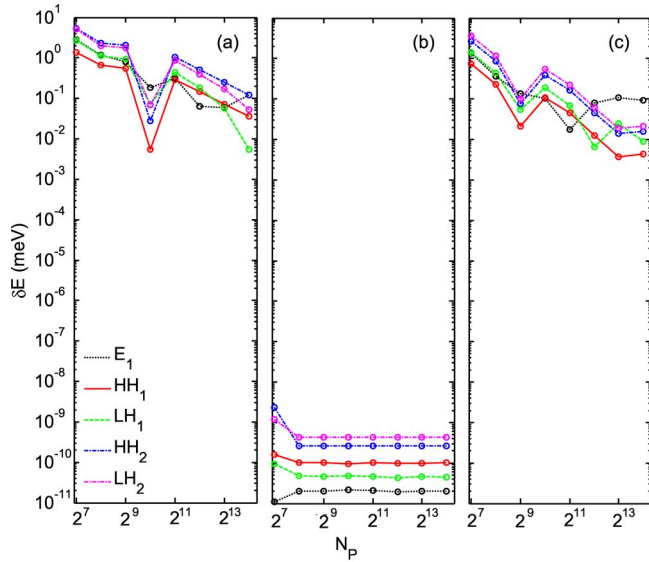


FIG. 5. (Color online) Discretization-caused numerical errors of eigensolutions ( $\mathbf{k}_{\parallel}=0$ ) versus the number of mesh points  $N_p$  for (a) AQW, (b) IQW, and (c) SSL.

Fig. 5, where the numerical errors are plotted versus the number of mesh points  $N_p$  with reference to the eigenvalue solutions at  $N_p=2^{15}$  and  $N=100$ . To reach an accuracy of  $\sim 1$  meV, the required  $N_p$  should be no less than 1024 and 256 for AQW and SSL, respectively. For the similar accuracy, the required  $N_p$  may be even less than 128 for IQW. Apparently, we see that for structures with abrupt interfaces and thus larger Fourier spectrum span, a larger number of mesh points is necessary.

#### IV. COMPARISON OF FTM AND FDM

In the FTM, accuracy may be influenced by the number of mesh points  $N_p$  and the truncation Fourier frequency  $N$ , but the number of mesh points is the only consideration for accuracy in the FDM. In Fig. 6, we plot the curves of the

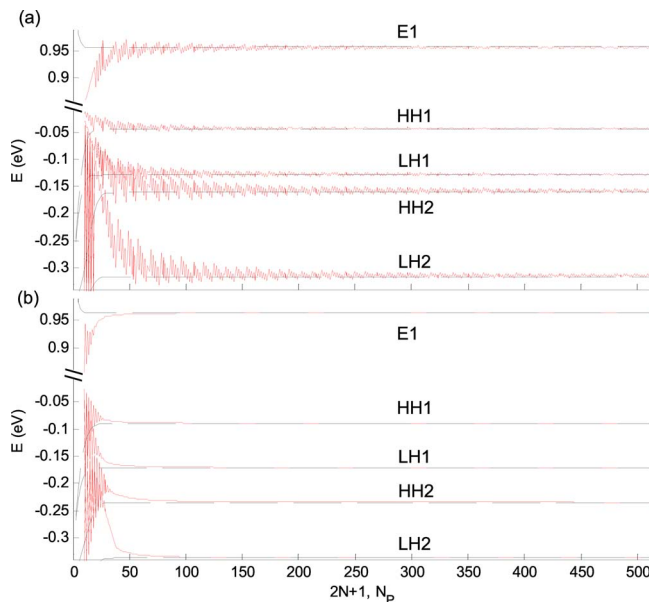


FIG. 6. (Color online) Eigenenergy solutions at  $\mathbf{k}_{\parallel}=0$  in (a) AQW and (b) IQW by the FTM (—) with respect to  $2N+1$  and the FDM (---) with respect to the number of mesh points.

eigenvalues versus  $N_p$  solved by the FDM and the eigenvalues versus  $2N+1$  solved by the FTM for AQW and IQW, respectively. Comparison is done under the same dimension of the Hamiltonian matrix.  $N_p$  influences the accuracy to a different extent for different heterostructures. The FDM curve for AQW in Fig. 6 shows zigzag patterns swinging in ranges of 3–7 meV even for  $N_p > 500$ . This is due to edge jitter of the mesh near abrupt interfaces along with increasing  $N_p$ , which is equivalent to the fluctuation of the well width. This phenomenon is not observable in a graded QW like IQW once  $N_p$  is sufficiently large.

However, to further improve the accuracy in the FDM, more mesh points have to be pursued. In reality, the challenge is that the matrix may become too big to solve, because the matrix dimension is determined by the number of mesh points, i.e.,  $VN_p \times VN_p$ . In contrast, the dimension of the Hamiltonian matrix used in the FTM [Eqs. (10) and (11)] is subjective to  $N$ , i.e.,  $V(2N+1) \times V(2N+1)$ . From the above results, it is seen that to reach an accuracy of  $\sim 1$  meV,  $N=20$  is sufficient for all three cases. When more mesh points are needed to reduce the discretization-caused error, the FTM only brings more computation volume to the FFT, for which the increase in computing time is trivial. Apparently the FTM is much more efficient than the FDM, especially in dealing with abrupt QWs, as has also been manifested in the practical computation.

#### V. FORMULATION FOR QD SUPERLATTICE

The FTM presents a simple and neat formulation for the QW superlattice in Eq. (11). It brings the same advantage to the QD superlattice as well. The envelope function for a QD superlattice is expressed as

$$\mathbf{F}(\mathbf{r}) = \frac{1}{\sqrt{L_x L_y L_z}} e^{ik_x x + ik_y y + ik_z z} \sum_{n_x=-N_x}^{N_x} \sum_{n_y=-N_y}^{N_y} \sum_{n_z=-N_z}^{N_z} \mathbf{c}_{n_x n_y n_z} \times e^{i(n_x \kappa_x x + n_y \kappa_y y + n_z \kappa_z z)}, \quad (13)$$

where  $L_x$ ,  $L_y$ , and  $L_z$  are the structural periods;  $\mathbf{c}_{n_x n_y n_z} = [c_1 c_2 \cdots c_8]_{n_x n_y n_z}^T$ ;  $\kappa_\alpha = 2\pi/L_\alpha$ ; and  $-\kappa_\alpha < k_\alpha < \kappa_\alpha$ .  $\alpha$  represents  $x$ ,  $y$ , and  $z$ .

The spatial domain Hamiltonian matrix is expressed in the Fourier domain using Fourier transform

$$\begin{aligned} \mathbf{H} &= \sum_{\alpha, \beta=x, y, z} \mathbf{H}^{\alpha\beta}(x, y, z) \widehat{k}_\alpha \widehat{k}_\beta \\ &+ \sum_{\alpha=x, y, z} \mathbf{H}^\alpha(x, y, z) \widehat{k}_\alpha + \mathbf{H}^0(x, y, z) \\ &= \sum_{\alpha, \beta} \sum_{q_x, q_y, q_z} \mathbf{H}^{\alpha\beta}(q_x, q_y, q_z) e^{i(q_x \kappa_x x + q_y \kappa_y y + q_z \kappa_z z)} \widehat{k}_\alpha \widehat{k}_\beta \\ &+ \sum_{\alpha} \sum_{q_x, q_y, q_z} \mathbf{H}^\alpha(q_x, q_y, q_z) e^{i(q_x \kappa_x x + q_y \kappa_y y + q_z \kappa_z z)} \widehat{k}_\alpha \\ &+ \sum_{q_x, q_y, q_z} \mathbf{H}^0(q_x, q_y, q_z) e^{i(q_x \kappa_x x + q_y \kappa_y y + q_z \kappa_z z)}. \end{aligned} \quad (14)$$

Denoting  $\langle f_2 | f_1 \rangle = 1/V \iiint_V f_2^* f_1 d\Omega$ , the eigenvalue equation  $\mathbf{H}\mathbf{F} = E\mathbf{F}$  gives

$$\begin{aligned}
& \sum_{\alpha, \beta} \sum_{q_x, q_y, q_z} \mathbf{H}_{q_x, q_y, q_z}^{\alpha\beta} e^{i(q_x \kappa_x x + q_y \kappa_y y + q_z \kappa_z z)} \widehat{k}_\alpha \widehat{k}_\beta \left( e^{ik_x x + ik_y y + ik_z z} \sum_{n_x=-N_x}^{N_x} \sum_{n_y=-N_y}^{N_y} \sum_{n_z=-N_z}^{N_z} \mathbf{c}_{n_x, n_y, n_z} e^{i(n_x \kappa_x x + n_y \kappa_y y + n_z \kappa_z z)} \right) \\
& + \sum_{\alpha} \sum_{q_x, q_y, q_z} \mathbf{H}_{q_x, q_y, q_z}^{\alpha} e^{i(q_x \kappa_x x + q_y \kappa_y y + q_z \kappa_z z)} \widehat{k}_\alpha \left( e^{ik_x x + ik_y y + ik_z z} \sum_{n_x=-N_x}^{N_x} \sum_{n_y=-N_y}^{N_y} \sum_{n_z=-N_z}^{N_z} \mathbf{c}_{n_x, n_y, n_z} e^{i(n_x \kappa_x x + n_y \kappa_y y + n_z \kappa_z z)} \right) \\
& + \sum_{q_x, q_y, q_z} \mathbf{H}_{q_x, q_y, q_z}^{(0)} e^{i(q_x \kappa_x x + q_y \kappa_y y + q_z \kappa_z z)} \left( e^{ik_x x + ik_y y + ik_z z} \sum_{n_x=-N_x}^{N_x} \sum_{n_y=-N_y}^{N_y} \sum_{n_z=-N_z}^{N_z} \mathbf{c}_{n_x, n_y, n_z} e^{i(n_x \kappa_x x + n_y \kappa_y y + n_z \kappa_z z)} \right) \\
& = E \left( e^{ik_x x + ik_y y + ik_z z} \sum_{n_x=-N_x}^{N_x} \sum_{n_y=-N_y}^{N_y} \sum_{n_z=-N_z}^{N_z} \mathbf{c}_{n_x, n_y, n_z} e^{i(n_x \kappa_x x + n_y \kappa_y y + n_z \kappa_z z)} \right). \tag{15}
\end{aligned}$$

With Hermitian operation, the matrix element for the eigenvalue equation [Eq. (10)] can be obtained,

$$\begin{aligned}
M = & \frac{1}{2} \sum_{\alpha, \beta}^{x, y, z} [2k_\alpha k_\beta + k_\alpha (m_\beta + n_\beta) \kappa_\beta + k_\beta (m_\alpha + n_\alpha) \kappa_\alpha \\
& + (m_\alpha n_\beta + m_\beta n_\alpha) \kappa_\alpha \kappa_\beta] H_{uv}^{\alpha\beta}(q_x, q_y, q_z) + \frac{1}{2} \sum_{\alpha}^{x, y, z} [2k_\alpha \\
& + (m_\alpha + n_\alpha) \kappa_\alpha] H_{uv}^{\alpha}(q_x, q_y, q_z) + H_{uv}^0(q_x, q_y, q_z), \tag{16}
\end{aligned}$$

where  $q_x = m_x - n_x$ ,  $q_y = m_y - n_y$ , and  $q_z = m_z - n_z$ .

## VI. CONCLUSION

We have presented the FTM for solving multiband  $k \cdot p$  eigenproblems of heterostructures. The Fourier domain Hamiltonian expressed in a simple and neat form is derived from the position-dependent Hamiltonian in a spatial domain. The dimension of the Hamiltonian used in the FTM is determined by the truncation frequency  $N$  only. In case analytical expressions of the Fourier series are not given, a dense mesh can be adopted to reduce the discretization-caused numerical error with trivial increase of computing time. Therefore, the FTM is numerically efficient in solving multiband  $k \cdot p$  eigenproblems. This advantage is more prominent for a heterostructure with abrupt interfaces. Approximation by adopting the QW layer's bulk Hamiltonian with a perturbation term for band offsets may lead to large deviation for

large  $k$  in long-period superlattices and even at zero  $k$  in short-period superlattices. Furthermore, the FTM presents a simple and neat formulation for the QD eigenproblems as well.

## ACKNOWLEDGMENTS

The author would like to thank D. Z.-Y. Ting and X. Cartoixà for useful discussions on FDM behaviors. This work is supported in part by the joint Research Grant (No. ARC 2/05) from the Ministry of Education (MOE) and the Agency for Science, Technology and Research (A\*STAR), Singapore.

- <sup>1</sup>J. Luttinger and W. Kohn, Phys. Rev. **97**, 869 (1955).
- <sup>2</sup>E. O. Kane, J. Phys. Chem. Solids **1**, 249 (1957).
- <sup>3</sup>D. L. Smith and C. Mailhot, Phys. Rev. B **33**, 8345 (1986).
- <sup>4</sup>Y. X. Liu, D. Z.-Y. Ting, and T. C. McGill, Phys. Rev. B **54**, 5675 (1996).
- <sup>5</sup>S. L. Chuang and C. S. Chang, Semicond. Sci. Technol. **12**, 252 (1997).
- <sup>6</sup>S. F. Tsay, J. C. Chiang, Z. M. Chau, and I. Lo, Phys. Rev. B **56**, 13242 (1997).
- <sup>7</sup>H. T. Johnson, L. B. Freund, C. D. Akyüz, and A. Zaslavsky, J. Appl. Phys. **84**, 3714 (1998).
- <sup>8</sup>G. Bastard and J. A. Brum, IEEE J. Quantum Electron. **22**, 1625 (1986).
- <sup>9</sup>M. G. Burt, Semicond. Sci. Technol. **2**, 460 (1987).
- <sup>10</sup>G. A. Baraff and D. Gershoni, Phys. Rev. B **43**, 4011 (1991).
- <sup>11</sup>T. B. Bahder, Phys. Rev. B **41**, 11992 (1990).
- <sup>12</sup>X. Cartoixà, D. Z.-Y. Ting, and T. C. McGill, J. Appl. Phys. **93**, 3974 (2003).
- <sup>13</sup>S. Ridene, K. Boujdaria, H. Bouchriha, and G. Fishman, Phys. Rev. B **64**, 085329 (2001).